Available online at www.sciencedirect.com
SCIENCE DIRECT®
Journal of Sound and Vibration 282 (2005) 881–898
JOURNAL OF SOUND AND VIBRATION
www.elsevier.com/locate/jsvi

Hunting stability analysis of high-speed railway vehicle trucks on tangent tracks

Sen-Yung Lee*, Yung-Chang Cheng

Department of Mechanical Engineering, National Cheng Kung University, Tainan, Taiwan 701, Republic of China

Received 27 May 2003; received in revised form 2 September 2003; accepted 15 March 2004

Abstract

Using the linear creep model, this paper derives the governing differential equations of motion for a truck moving on tangent tracks. The truck is modeled by a 10 degree-of-freedom (DOF) system which considers the lateral displacement, vertical displacement, roll angle and yaw angle of each wheelset and the lateral displacement and yaw angle of the truck frame. It is shown that the critical hunting speeds evaluated using the 10-DOF system differ significantly from those calculated using a system with six-DOF. The influences on the critical hunting speeds of certain physical parameters not considered in the six-DOF system are evaluated for wheels of different conicities. The accuracy of the present analysis is verified by comparing the limiting case and the current numerical results with the findings available in published literature.

1. Introduction

High-speed railway (HSR) vehicles are assuming an ever-increasing importance in today's transportation infrastructures. With the advent of high-speed passenger trains in Japan, Europe and America, the problem of achieving a high-speed operation without hunting instability has become a matter of pressing concern for vehicle designers around the world.

The hunting phenomenon often occurs when railway vehicles are run at high speeds, and represents a coupled oscillation of the wheelset in its lateral displacement and yaw angle. Many

*Corresponding author. Fax: +886-6-235-2973.
E-mail address: sylee@mail.ncku.edu.tw (S.-Y. Lee).

0022-460X/$ - see front matter © 2004 Elsevier Ltd. All rights reserved.
doi:10.1016/j.jsv.2004.03.050

Nomenclature

a half of track gauge
b_1 half of the primary yaw spring arm and the primary yaw damping arm
b_1 half of the primary vertical spring arm and the primary vertical damping arm
b_2 half of the secondary longitudinal spring arm
b_3 half of the secondary longitudinal damping arm
C_{px} yaw damping of the primary suspension
C_{py} lateral damping of the primary suspension
C_{pz} vertical damping of the primary suspension
C_{sx} yaw damping of the secondary suspension
C_{sy} lateral damping of the secondary suspension
D_{v1} time response of front wheelset in the vertical direction
f_{11} lateral creep force coefficient
f_{12} lateral/spin creep force coefficient
f_{22} spin creep force coefficient
f_{33} longitudinal creep force coefficient
F^*_{jxi} linear creep force of front and rear wheelset ($i=1$, 2, respectively) as given directly by Kalker's linear theory in longitudinal direction of left and right wheel ($j=L$, R, respectively)
F^*_{jyi} linear creep force of front and rear wheelset ($i=1$, 2, respectively) as given directly by Kalker's linear theory in lateral direction of left and right wheel ($j=L$, R, respectively)
F_{Lxi} linear creep force of front and rear wheelset ($i=1$, 2, respectively) in longitudinal direction of left wheel
F_{Lyi} linear creep force of front and rear wheelset ($i=1$, 2, respectively) in lateral direction of left wheel
F_{Lzi} linear creep force of front and rear wheelset ($i=1$, 2, respectively) in vertical direction of left wheel
F_{Rxi} linear creep force of front and rear wheelset ($i=1$, 2, respectively) in longitudinal direction of right wheel
F_{Ryi} near creep force of front and rear wheelset ($i=1$, 2, respectively) in lateral direction of right wheel
F_{Rzi} linear creep force of front and rear wheelset ($i=1$, 2, respectively) in vertical direction of right wheel
F_{syi} suspension force of front and rear wheelset ($i=1$, 2, respectively) in lateral direction
F_{syt} suspension force of truck frame in lateral direction
F_{szi} suspension force of front and rear wheelset ($i=1$, 2, respectively) in vertical direction
F_{ti} flange contact force
h_f wheel flange height
h_T vertical distance from the wheelset center of gravity to the secondary suspension
I_{tz} yaw moment of inertia of the truck
I_{wx} roll moment of inertia of the wheelset
I_{wy} spin moment of inertia of the wheelset
I_{wz} yaw moment of inertia of the wheelset
K_r lateral rail stiffness
K_{px} longitudinal stiffness of the primary suspension
K_{py} lateral stiffness of the primary suspension
K_{pz} vertical stiffness of the primary suspension
K_{sx} longitudinal stiffness of the secondary suspension
K_{sy} lateral stiffness of the secondary suspension
L_1 half of the primary lateral spring arm
L_2 half of the primary lateral damping arm
m_t bogie frame mass
m_w wheelset mass
M^*_{jzi} linear creep moment of front and rear wheelset ($i=1$, 2, respectively) as given directly by Kalker's linear theory in vertical direction of left and right wheel ($j=L$, R, respectively)

M_{Lxi}	linear creep moment of front and rear wheelset ($i=1$, 2, respectively) in longitudinal direction on left wheel
M_{Lzi}	linear creep moment of front and rear wheelset ($i=1$, 2, respectively) in vertical direction on left wheel
M_{Rxi}	linear creep moment of front and rear wheelset ($i=1$, 2, respectively) in longitudinal direction on right wheel
M_{Rzi}	linear creep moment of front and rear wheelset ($i=1$, 2, respectively) in vertical direction on right wheel
M_{sxi}	suspension moment of front and rear wheelset ($i=1$, 2, respectively) in longitudinal direction
M_{szi}	suspension moment of front and rear wheelset ($i=1$, 2, respectively) in vertical direction
M_{szt}	suspension moment of truck frame in vertical direction
N	normal force of wheelset at the equilibrium state
N_{Lyi}	normal force on left wheel of front and rear wheelset ($i=1$, 2, respectively) in lateral direction
N_{Lzi}	normal force on left wheel of front and rear wheelset ($i=1$, 2, respectively) in vertical direction
N_{Ryi}	normal force on right wheel of front and rear wheelset ($i=1$, 2, respectively) in lateral direction
N_{Rzi}	normal force on right wheel of front and rear wheelset ($i=1$, 2, respectively) in vertical direction
r_L	left wheel rolling radius
r_R	right wheel rolling radius
r_0	nominal wheelset rolling radius
R_{Lxi}	x component of position vector on left wheel of front and rear wheelset ($i=1$, 2, respectively)
R_{Lyi}	y component of position vector on left wheel of front and rear wheelset ($i=1$, 2, respectively)
R_{Rxi}	x component of position vector on right wheel of front and rear wheelset ($i=1$, 2, respectively)
R_{Ryi}	y component of position vector on right wheel of front and rear wheelset ($i=1$, 2, respectively)
t	time
V	forward speed of truck
V_{cr}	critical hunting speed
W	axle load
x	longitudinal coordinate
y	lateral coordinate
y_i	lateral displacement of front and rear wheelset ($i=1$, 2, respectively)
y_t	lateral displacement of truck
z	vertical coordinate
z_i	vertical displacement of front and rear wheelset ($i=1$, 2, respectively)
Δ_L	lateral displacement of the contact points from their equilibrium position of left wheel
Δ_R	lateral displacement of the contact points from their equilibrium position of right wheel
δ	flange clearance between the wheel and the rail
δ_L	contact angle of left wheel
δ_R	contact angle of right wheel
λ	wheel conicity
ϕ_i	roll angle of front and rear wheelset, respectively ($i=1$, 2, respectively)
ψ_i	yaw angle of front and rear wheelset, respectively ($i=1$, 2, respectively)
ψ_t	yaw angle of truck

investigations concerning the hunting stability of trucks running on tangent tracks are to be found in the published literature [1–14]. An early survey on this subject was presented by Law and Cooperrider [2]. Early investigations into the hunting stability of a truck generally modeled the truck system by a four or six degrees-of-freedom (DOF) system. Studies considering a four degrees-of-freedom (DOF) system, i.e. one which considers the lateral displacement and yaw

angle of each wheelset, include those by Wickens [3,4], Whitman [5], Whitman and Molyneux [6], and Dukkipati et al. [7]. Meanwhile, the hunting stability of a truck modeled by a six-DOF system, i.e. a system considering the lateral displacement and yaw angle of the two wheelsets and of the truck frame, has been investigated by Horak and Wormley [8], Nó and Hedrick [9], Piotrowski [10], Haque and Lieh [11], Narayana et al. [12], Dukkipati et al. [13], and Mehdi and Shaopu [14].

The relationship between the damping and the critical hunting speed of a truck has been studied by Wickens [3]. Wickens [4] also illustrated the boundaries of the hunting stability as functions of the suspension stiffness for trucks with linkage steered wheelsets. Deliberately neglecting the mass of the truck frame, various researchers have investigated the influences of wheelset bending and wheelset shear stiffness on the critical hunting speed of a truck, including Whitman [5], Whitman and Molyneux [6], Piotrowski [10], Dukkipati et al. [7,13], and Narayana et al. [12]. Horak and Wormley [8] studied the influence of wheel conicity on the critical hunting speed of a rail passenger truck running on irregularly aligned rails. Nó and Hedrick [9] illustrated the influences on the critical hunting speed of a railway vehicle of the lateral and longitudinal stiffness of the primary suspension and of the longitudinal damping of the secondary suspension. Utilizing the Bogoliubov averaging method and the perturbation method, Mehdi and Shaopu [14] investigated the influences of suspension parameters on the critical hunting speed of a truck for the case of nonlinear damping forces. Finally, Haque and Lieh [11] employed the Floquet theory to examine the parametric hunting stabilities of a passenger truck and a freight truck running on tangent tracks for harmonic variations in the wheel conicity.

An important aspect of the hunting analysis for HSR vehicle systems is the consideration of the vertical and roll motions of the wheelsets. However, a review of the existing literature reveals that previous studies into the hunting stability of a truck moving on tangent tracks have never adopted the 10-DOF systems required to take these two parameters into consideration. Moreover, even though the equations of motion for a 10-DOF system were established by Dukkipati and Garg [1], the flange contact forces were still not considered. Additionally, the creep and suspension forces in the vertical direction and the creep and suspension moments in the longitudinal direction of the two wheelsets were also neglected.

This paper adopts Kalker's linear theory to derive the governing differential equations of motion for a truck modeled by a 10-DOF system moving on tangent tracks. To verify the accuracy of the present analysis, the limiting case and the numerical results are compared with the findings available in published literature. In order to ensure that the wheels do not lose contact with the rails, the maximum vertical displacements of the wheels are restricted to be less than the height of the wheel flange. Using the Runge–Kutta fourth-order method, the time responses of the lateral displacement and the yaw angle of the front wheelset are calculated to illustrate the dynamic behavior of the system when the truck speed is less than, equal to, and greater than the critical hunting speed. The Lyapunov indirect method is utilized to evaluate and compare the influences of several physical parameters on the critical hunting speeds for the six-DOF and 10-DOF systems. Finally, the influences on the critical hunting speeds of the primary suspension vertical stiffness and vertical damping physical parameters, which are not considered in the six-DOF system, are investigated for different wheel conicities.

2. Differential equations of motion

Figs. 1 and 2 illustrate the truck system considered in the present study. The governing differential equations of motion for the lateral displacement, y_t, and the yaw angle, ψ_t, of the truck frame are given by

$$m_t\ddot{y}_t = F_{syt}, \tag{1}$$

$$I_{tz}\ddot{\psi}_t = M_{szt}, \tag{2}$$

where the physical quantities F_{syt}, I_{tz}, M_{szt}, and m_t are defined in the nomenclature. It is noted that in Eqs. (1) and (2), the dots indicate differentiation with respect to the time variable t.

Adopting the notations used by Dukkipati and Garg [1], the governing differential equations of motion for the lateral displacement, y_i, the vertical displacement, z_i, the roll angle, ϕ_i, and the yaw

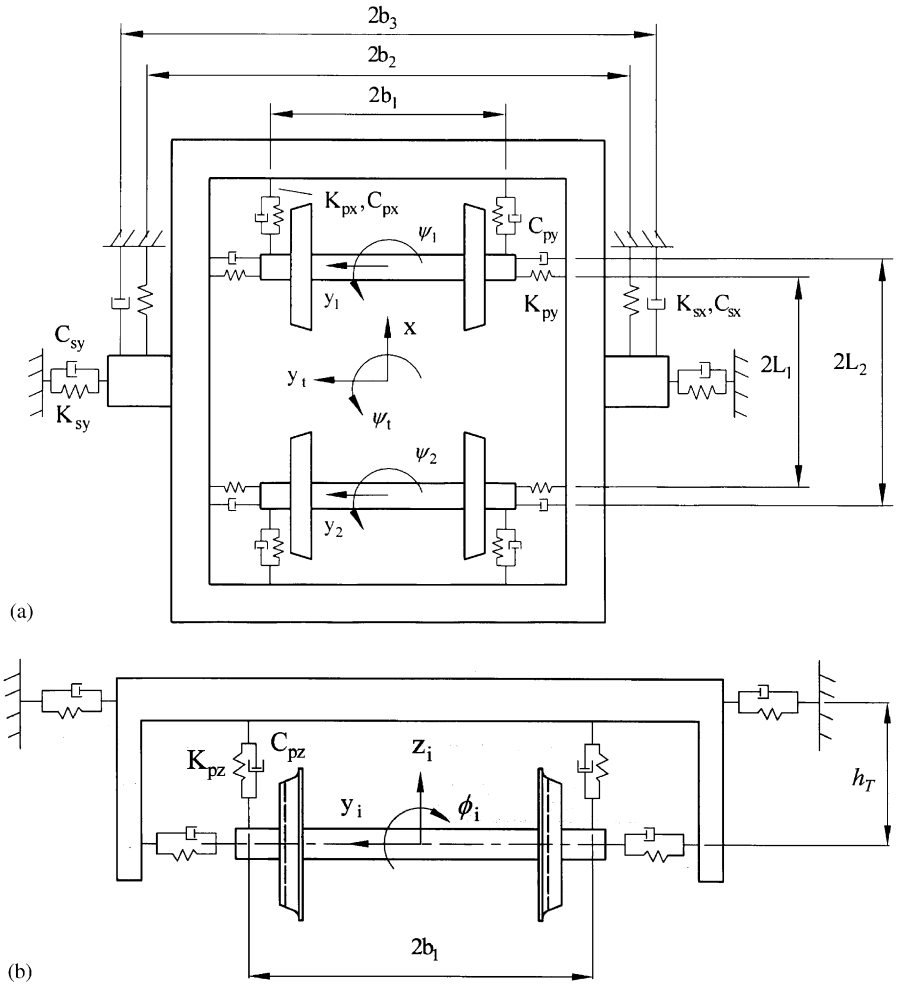

Fig. 1. Two-axle truck model.

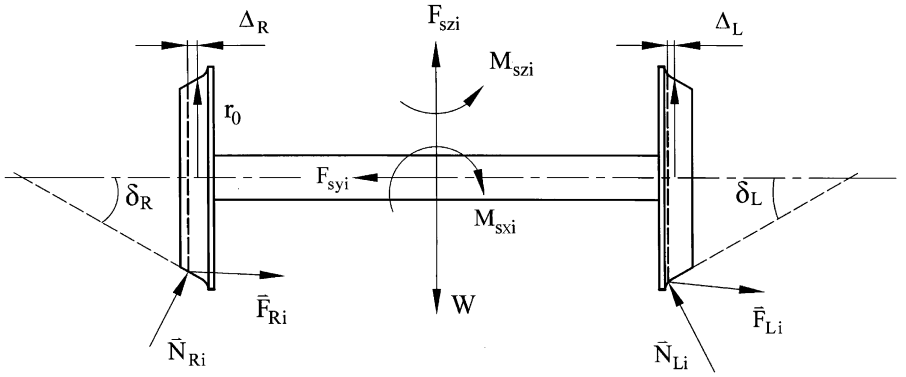

Fig. 2. Free-body diagram of a single wheelset.

angle, ψ_i, of the wheelsets are given by

$$m_w\ddot{y}_i = F_{Lyi} + F_{Ryi} + N_{Lyi} + N_{Ryi} + F_{syi} - F_{ti}, \tag{3}$$

$$m_w\ddot{z}_i = F_{Lzi} + F_{Rzi} + N_{Rzi} + N_{Lzi} + F_{szi} - W, \tag{4}$$

$$\begin{aligned} I_{wx}\ddot{\phi}_i = {} & I_{wy}\frac{V}{r_0}\dot{\psi}_i + (R_{Ryi}F_{Rzi} - R_{Rzi}F_{Ryi}) + R_{Lyi}F_{Lzi} - R_{Lzi}F_{Lyi}) \\ & + (R_{Lyi}N_{Lzi} + R_{Ryi}N_{Rzi}) - (R_{Rzi}N_{Ryi} + R_{Lzi}N_{Lyi}) \\ & + M_{Lxi} + M_{Rxi} + M_{sxi}, \end{aligned} \tag{5}$$

$$\begin{aligned} I_{wz}\ddot{\psi}_i = {} & -I_{wy}\frac{V}{r_0}\dot{\phi}_i + (R_{Rxi}F_{Ryi} - R_{Ryi}F_{Rxi}) + (R_{Lxi}F_{Lyi} - R_{Lyi}F_{Lxi}) \\ & + (R_{Rxi}N_{Ryi} + R_{Lxi}N_{Lyi}) + M_{Lzi} + M_{Rzi} + M_{szi}. \end{aligned} \tag{6}$$

It is noted that in these equations (and throughout the remainder of the paper), the subscripts $i=1$ and 2 denote the front and the rear wheelset, respectively. In Eqs. (5) and (6), V indicates the forward speed of the truck. Meanwhile, the physical parameters F_{Lxi}, F_{Lyi}, F_{Lzi}, F_{Rxi}, F_{Ryi}, F_{Rzi}, F_{syi}, F_{szi}, F_{ti}, I_{wx}, I_{wy}, I_{wz}, M_{Lxi}, M_{Lzi}, M_{Rxi}, M_{Rzi}, M_{sxi}, M_{szi}, m_w, N_{Lyi}, N_{Lzi}, N_{Ryi}, N_{Rzi}, r_0, R_{Lxi}, R_{Lyi}, R_{Lzi}, R_{Rxi}, R_{Ryi}, and R_{Rzi}, are all defined in the nomenclature. In Eq. (3), F_{ti} indicates the flange contact force.

If the roll and yaw angles of each wheelset are assumed to be small, the various linear creep forces and linear creep moments with respect to the left wheel and the right wheel are given by

$$F_{Lxi} = F^*_{Lxi} - F^*_{Lyi}\psi_i, \tag{7a}$$

$$F_{Lxi} = F^*_{Lxi}\psi_i - F^*_{Lyi}, \tag{7b}$$

$$F_{Lzi} = F^*_{Lyi}(\delta_L + \phi_i), \tag{7c}$$

$$M_{Lxi} = M^*_{Lzi}(\delta_L + \phi_i)\psi_i, \tag{7d}$$

$$M_{Lzi} = M^*_{Lzi}, \tag{7e}$$

$$F_{Rxi} = F^*_{Rxi} - F^*_{Ryi}\psi_i, \tag{8a}$$

$$F_{Ryi} = F^*_{Rxi}\psi_i + F^*_{Ryi}, \tag{8b}$$

$$F_{Rzi} = -F^*_{Ryi}(\delta_R - \phi_i), \tag{8c}$$

$$M_{Rxi} = -M^*_{Rzi}(\delta_R - \phi_i)\psi_i, \tag{8d}$$

$$M_{Rzi} = M^*_{Rzi}, \tag{8e}$$

where the creep forces, F^*_{jxi} and F^*_{jyi}, and the creep moment, M^*_{jzi} $(j = R, L)$, are calculated from Kalker's linear theory, i.e.

$$F^*_{Lxi} = -\frac{f_{33}}{V}\left[V\left(1 - \frac{r_L}{r_0}\right) - a\dot{\psi}_i\right], \tag{9a}$$

$$F^*_{Lyi} = -\frac{f_{11}}{V}\left[\dot{y}_i + r_L\dot{\phi}_i - V\psi_i\right] - \frac{f_{12}}{V}\left[\dot{\psi}_i - \frac{V}{r_0}\delta_L\right], \tag{9b}$$

$$M^*_{Lzi} = \frac{f_{12}}{V}[\dot{y}_i + r_L\dot{\phi}_i - V\psi_i] - \frac{f_{22}}{V}\left[\dot{\psi}_i - \frac{V}{r_0}\delta_L\right], \tag{9c}$$

$$F^*_{Rxi} = -\frac{f_{33}}{V}\left[V\left(1 - \frac{r_R}{r_0}\right) - a\dot{\psi}_i\right], \tag{9d}$$

$$F^*_{Ryi} = -\frac{f_{11}}{V}\left[\dot{y}_i + r_R\dot{\phi}_i - V\psi_i\right] - \frac{f_{12}}{V}\left[\dot{\psi}_i - \frac{V}{r_0}\delta_R\right], \tag{9e}$$

$$M^*_{Rzi} = \frac{f_{12}}{V}[\dot{y}_i + r_R\dot{\phi}_i - V\psi_i] - \frac{f_{22}}{V}\left[\dot{\psi}_i - \frac{V}{r_0}\delta_R\right]. \tag{9f}$$

From the static force equilibrium in the vertical direction, the normal forces of the left and right wheel in the vertical direction, N_{Lzi} and N_{Rzi}, are given by

$$N_{Lzi} = N_{Rzi} = \tfrac{1}{2}W. \tag{10}$$

Meanwhile, the normal forces of the left and right wheel in the lateral direction, N_{Lyi} and N_{Rzi}, are obtained from:

$$\begin{aligned} N_{Lyi} &= -N_{Lzi}\tan(\delta_L + \phi_i) \\ &\approx -\tfrac{1}{2}W(\delta_L + \phi_i), \end{aligned} \tag{11}$$

and

$$N_{Ryi} = N_{Rzi}\tan(\delta_R + \phi_i) \approx \tfrac{1}{2}W(\delta_R - \phi_i). \tag{12}$$

Assuming that the displacements of the contact points from their equilibrium positions, Δ_L and Δ_R, are small, then the position vectors of these points are

$$R_{Rxi} = a\psi_i, \tag{13a}$$

$$R_{Ryi} = -a + r_R\phi_i, \tag{13b}$$

$$R_{Rzi} = -a\phi_i - r_R, \tag{13c}$$

$$R_{Lxi} = -a\psi_i, \tag{13d}$$

$$R_{Lyi} = a + r_L\phi_i, \tag{13e}$$

$$R_{Lzi} = a\phi_i - r_L. \tag{13f}$$

Eqs. (10)–(13) enable the summation moments in the longitudinal direction, i.e. $R_{Ryi}N_{Rzi}+R_{Lyi}N_{Lzi}$ and $-R_{Rzi}N_{Ryi}-R_{Lzi}N_{Lyi}$, and in the vertical direction, i.e. $R_{Rxi}N_{Ryi}+R_{Lxi}N_{Lyi}$, to be obtained.

From Fig. 1, it can be shown that the suspension forces of the wheelsets in the lateral direction, F_{syi}, the suspension moments of the wheelsets in the vertical direction, M_{szi}, the suspension forces of the truck frame, F_{syt}, and the suspension moments of the truck frame, M_{szt}, are given by

$$F_{syi} = -2K_{py}y_i - (-1)^i 2K_{py}L_1\psi_t + 2K_{py}y_t - 2C_{py}\dot{y}_i - (-1)^i 2C_{py}L_2\dot{\psi}_t + 2C_{py}\dot{y}_t, \tag{14a}$$

$$M_{szi} = 2K_{px}b_1^2\psi_t - 2K_{px}b_1^2\psi_i + 2C_{px}b_1^2\dot{\psi}_t - 2C_{px}b_1^2\dot{\psi}_i, \tag{14b}$$

$$F_{syt} = 2K_{py}y_1 + 2C_{py}\dot{y}_1 + 2K_{py}y_2 + 2C_{py}\dot{y}_2 + (-4K_{py} - 2K_{sy})y_t + (-4C_{py} - 2C_{sy})\dot{y}_t, \tag{14c}$$

$$\begin{aligned} M_{szt} = {} & (-4K_{py}L_1^2 - 4K_{px}b_1^2 - 2K_{sx}b_2^2)\psi_t \\ & + (-4C_{py}L_2^2 - 4C_{px}b_1^2 - 2C_{sx}b_3^2)\dot{\psi}_t \\ & + 2K_{py}L_1y_1 + 2C_{py}L_2\dot{y}_1 + 2K_{px}b_1^2\psi_1 + 2C_{px}b_1^2\dot{\psi}_1 \\ & - 2K_{py}L_1y_2 - 2C_{py}L_2\dot{y}_2 + 2K_{px}b_1^2\psi_2 + 2C_{px}b_1^2\dot{\psi}_2. \end{aligned} \tag{14d}$$

Other than Eqs. (7c), (7d), (8c) and (8d), the physical quantities given by Eqs. (7)–(14) are given by, or easily reduced from, the expressions established previously by Dukkipati and Garg [1], who neglected the vertical stiffness and vertical damping of the primary suspension in their system. F_{Lzi} and F_{Rzi} in Eqs. (7c) and (8c), respectively, are the creep forces of the left and right wheels in the vertical direction, respectively. Meanwhile, M_{Lxi} and M_{Rxi} in Eqs. (7d) and (8d), respectively, are the creep moments of the left and right wheels in the longitudinal direction, respectively.

From Fig. 1, the suspension forces in the vertical direction, F_{szi}, and the suspension moments in the longitudinal direction, M_{sxi}, acting on the wheelsets are induced from the vertical stiffness and

vertical damping of the primary suspension, and can be expressed as

$$F_{szi} = -2K_{pz}z_i - 2C_{pz}\dot{z}_i, \tag{15a}$$

and

$$M_{sxi} = -2K_{sy}h_T y_t - 2C_{sy}h_T\dot{y}_t - 2b_1^2K_{pz}\phi_i - 2b_1^2C_{pz}\dot{\phi}_i, \tag{15b}$$

respectively. The flange contact force, F_{ti}, is given by Mehdi and Shaopu [14]) as

$$F_{ti} = \begin{cases} K_r(y_i - \delta), & y_i > \delta, \\ 0, & -\delta \leqslant y_i \leqslant \delta, \\ -K_r(y_i + \delta), & y_i < -\delta, \end{cases} \tag{16}$$

where δ is the flange clearance between the wheel and the rail.

For simplicity, it is assumed that the constraint function is linear for a conical wheel on a knife-edged rail. Hence, the following assumptions regarding the wheel and rail geometry can be employed:

$$\delta_L = \delta_R = \lambda, \quad \tfrac{1}{2}(r_L - r_R) = \lambda y_i, \quad \tfrac{1}{2}(r_L + r_R) = r_0. \tag{17}$$

Substituting the equations given above into Eqs. (3)–(6) and neglecting the high-order terms yields the following differential equations:

$$m_w\ddot{y}_i = -\frac{2f_{11}}{V}\dot{y}_i + 2f_{11}\psi_i - \frac{2f_{12}}{V}\dot{\psi}_i - W\phi_i - \frac{2r_0f_{11}}{V}\dot{\phi}_i + F_{syi} - F_{ti}, \tag{18}$$

$$m_w\ddot{z}_i = -\frac{2f_{11}}{V}\lambda^2\dot{\phi}y_i - \frac{2f_{11}}{V}\phi_i\dot{y}_i - \frac{2f_{12}}{V}\phi_i\dot{\psi}_i - \frac{2f_{11}r_0}{V}\dot{\phi}_i\phi_i + \frac{2f_{12}}{r_0}\lambda^2 + F_{szi}, \tag{19}$$

$$\begin{aligned} I_{wx}\ddot{\phi}_i = {} & \left(\frac{2f_{12}\lambda^2}{r_0}\lambda^2 W\right)y_i - \frac{2f_{11}(r_0 + a\lambda)}{V}\dot{y}_i \\ & + \left[2f_{11}(r_0 + a\lambda) + \frac{2f_{22}\lambda^2}{r_0}\right]\psi_i + \left(\frac{I_{wy}V}{r_0} - \frac{2f_{12}r_0}{V} - \frac{2f_{12}a\lambda}{V}\right)\dot{\psi}_i \\ & + (2\lambda^2 f_{12} + a\lambda W)\phi_i - \left[\frac{2f_{11}ar_0\lambda}{V} + \frac{2f_{11}r_0^2}{V}\right]\dot{\phi}_i + M_{sxi} \end{aligned} \tag{20}$$

$$\begin{aligned} I_{wz}\ddot{\psi}_i = {} & \frac{2a\lambda f_{33}}{r_0}y_i + \frac{2f_{12}}{V}\dot{y}_i + (-2f_{12} + a\lambda W)\psi_i \\ & - \left(\frac{2a^2f_{33}}{V} + \frac{2f_{22}}{V}\right)\dot{\psi}_i + \left[-\frac{I_{wy}V}{r_0} + \frac{2r_0f_{12}}{V}\right]\dot{\phi}_i + M_{szi}. \end{aligned} \tag{21}$$

Eqs. (1)–(2) and (18)–(21) form the 10 governing differential equations of motion for the system. When the vertical displacement and the roll angle of the wheelset are neglected and $\phi_i = \lambda y_i/a$,

Eqs. (18)–(21) can be reduced to

$$m_w\ddot{y}_i = -\frac{2f_{11}}{V}\dot{y}_i + 2f_{11}\psi_i - \frac{2f_{12}}{V}\dot{\psi}_i - W\frac{\lambda}{a}y_i - \frac{2r_0f_{11}}{V}\left(\frac{\lambda}{a}\right)\dot{y}_i + F_{syi} - F_{ti}, \tag{22}$$

$$\begin{aligned} I_{wz}\ddot{\psi}_i = & -\frac{2a\lambda f_{33}}{r_0}y_i + \frac{2f_{12}}{V}\dot{y}_i + (-2f_{12} + a\lambda W)\psi_i \\ & - \left(\frac{2a^2f_{33}}{V} + \frac{2f_{22}}{V}\right)\dot{\psi}_i + \left[-\frac{I_{wy}V}{r0} + \frac{2r_0f_{12}}{V}\right]\left(\frac{\lambda}{a}\right)\dot{y}_i + M_{szi}. \end{aligned} \tag{23}$$

Eqs. (1) and (2) and (22) and (23) are the governing differential equations of the motion of a truck modeled by a six-DOF system. It is noted that these equations are identical to those given previously by Mehdi and Shaopu [14].

3. Stability analysis

This paper utilizes the Lyapunov indirect method [15] to study the influence of the physical parameters on the critical hunting speed of a truck. The equations of motion of this autonomous system, i.e. Eqs. (1) and (2) and (18)–(21), can be re-expressed as a system of first-order differential equations, i.e.

$$\dot{\mathbf{x}}(t) = \mathbf{f}[\mathbf{x}(t)], \tag{24}$$

where $\mathbf{x}(t)$ is a 20×1 vector of state variables.

For any given velocity V, a determinant matrix $\mathbf{A}$ is defined as

$$\mathbf{A} = \left[\frac{\partial \mathbf{f}(\mathbf{x})}{\partial \mathbf{x}}\right]_{\mathbf{x}=\mathbf{x}_0}, \tag{25}$$

where $\mathbf{x}_0$ is the equilibrium point and satisfies $\mathbf{f}[\mathbf{x}_0] = 0$.

This dynamic system will be unstable if any one of the eigenvalues of matrix $\mathbf{A}$ has a positive real part. The lowest velocity for which the eigenvalues of the associated determinant matrix $\mathbf{A}$ has a non-positive real part corresponds to the critical hunting speed.

4. Numerical results

To verify the reliability of the current numerical analysis, the critical hunting speed of a truck modeled by a six-DOF system moving on a tangent track is compared with that calculated by Mehdi and Shaopu [14]. The critical hunting speed obtained in the present analysis is found to be 118 km/h, which corresponds exactly to the value determined by Mehdi and Shaopu [14].

Using the system data parameters listed in Appendix A [16,17], the influences of these physical parameters on the critical hunting speed are investigated for a freight truck. The maximum critical hunting speed of this truck system is found to be 410 km/h.

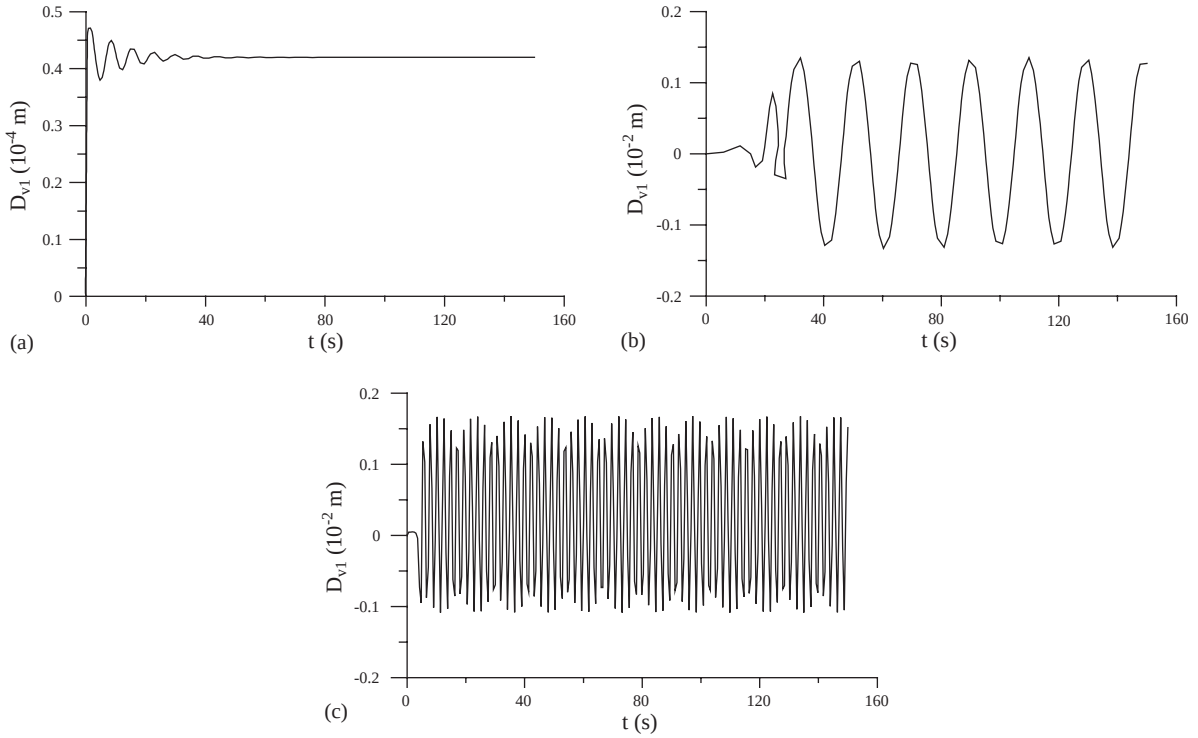

Fig. 3. Time response of front wheelset in vertical direction at: (a) $V=390$ km/h, (b) $V=410$ km/h, and (c) $V=500$ km/h.

Fig. 3 presents the time-varying displacement response of the right-front wheelset in the vertical direction, i.e. D_{V1} ($D_{V1}=z_1+a_1$), as calculated using the Runge–Kutta fourth-order method. The results indicate that the maximum vertical displacement of the wheel is less than 2 mm, which is significantly less than the height of the wheel flange (30 mm). Since the structure of the truck is symmetric with respect to the x- and y_t-coordinates, it can be concluded that the wheels will not lose contact with the rails.

Figs. 4 and 5 illustrate the lateral displacement and yaw angle, respectively, of the front wheelset for truck speeds of less than, equal to, and greater than the critical hunting speed. The results indicate that when the truck speed is less than the critical hunting speed, the truck system is stable and the dynamic responses of the front wheel set are asymptotically stable. Furthermore, when the truck moves at the critical hunting speed, i.e. $V=410$ km/h, the truck system is in a critical stable state and the dynamic responses of the front wheelset oscillate regularly. However, when the truck speed exceeds the critical hunting speed, the truck system becomes unstable and the dynamic responses of the front wheelset oscillate irregularly.

Figs. 6–9 compare the influences of various physical parameters on the critical hunting speeds for the six-DOF and 10-DOF systems. Fig. 6 reveals that the critical hunting speed initially increases to a maximum value as the longitudinal stiffness of the primary suspension, K_{px}, is increased, and then decreases as K_{px} is further increased. It is observed that the critical hunting speeds evaluated by the six-DOF system always exceed those evaluated by the 10-DOF system.

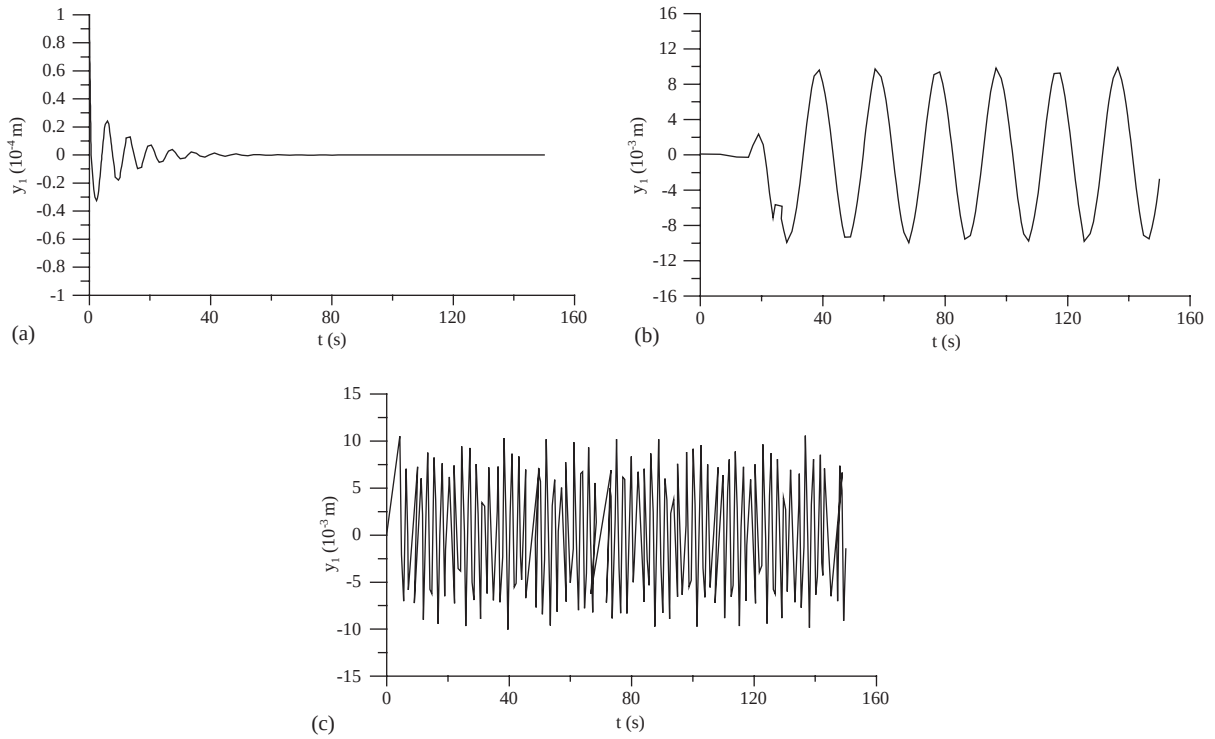

Fig. 4. Time response of lateral displacement of front wheelset at: (a) $V=390$ km/h, (b) $V=410$ km/h, and (c) $V=500$ km/h.

For low values of K_{px}, the difference between the two sets of critical hunting speeds is small. The results also indicate that the maximum critical hunting speed occurs at approximately the same value of K_{px} regardless of the modeling system employed.

Fig. 7 reveals that the influence on the critical hunting speeds of the lateral stiffness of the primary suspension, K_{py}, depends upon the particular modeling system considered. In the case of the 10-DOF system, the critical hunting speed is seen to be highly dependent on the lateral stiffness of the primary suspension when K_{py} is small. It is observed that the critical hunting speeds evaluated by the six-DOF system are always higher than those evaluated by the 10-DOF system. Moreover, the value of K_{py} which yields the maximum critical hunting speed is clearly higher in the case of the six-DOF system than in the 10-DOF system.

Fig. 8 illustrates the influence of the longitudinal damping of the secondary suspension, C_{sx}, on the critical hunting speeds for the six-DOF and 10-DOF systems. It is observed that when C_{sx} is small, the critical hunting speeds evaluated from the six-DOF system exceed those of the 10-DOF system. However, this relationship is inverted when C_{sx} is large.

Fig. 9 demonstrates that the lateral damping of the secondary suspension, C_{sy}, has only marginal influence on the critical hunting speeds when the six-DOF system is applied. However, in the case of the 10-DOF system, the critical hunting speed clearly increases as C_{sy} is increased. Furthermore, it is noted that the critical hunting speeds evaluated using the six-DOF system always exceed those evaluated by the 10-DOF system.

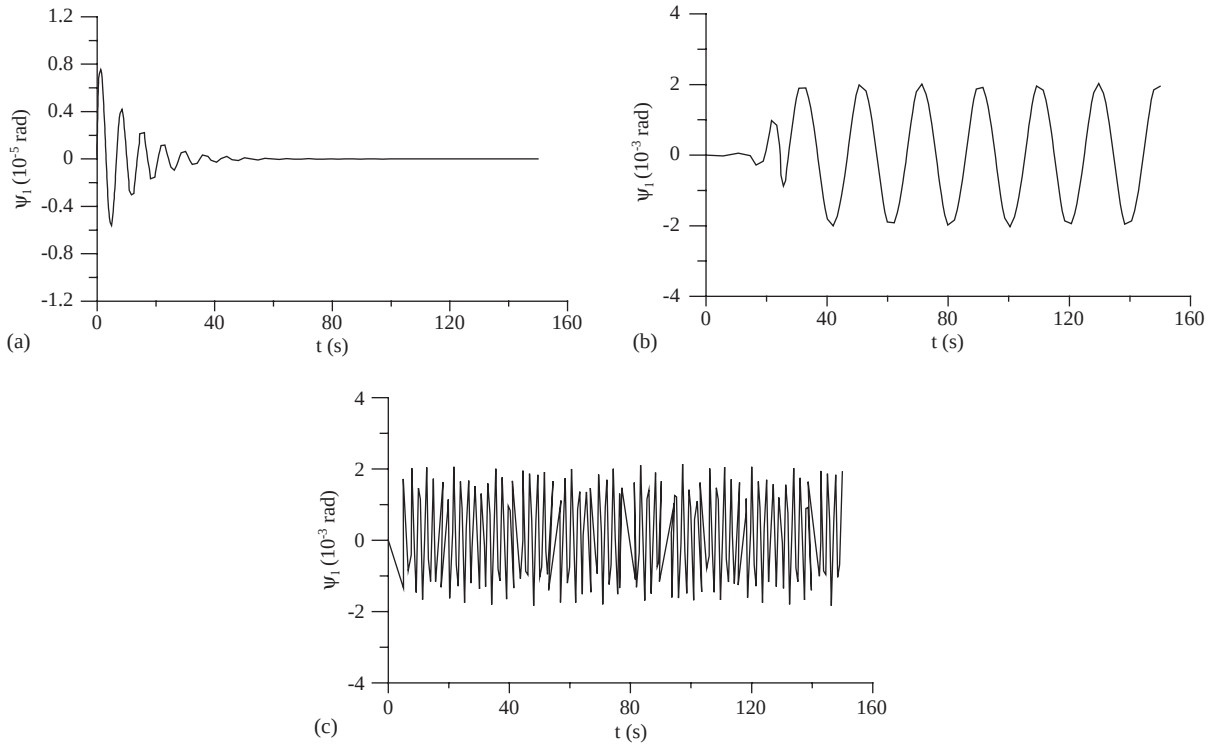

Fig. 5. Time response of yaw of angle of front wheelset at: (a) $V=390$ km/h, (b) $V=410$ km/h, and (c) $V=500$ km/h.

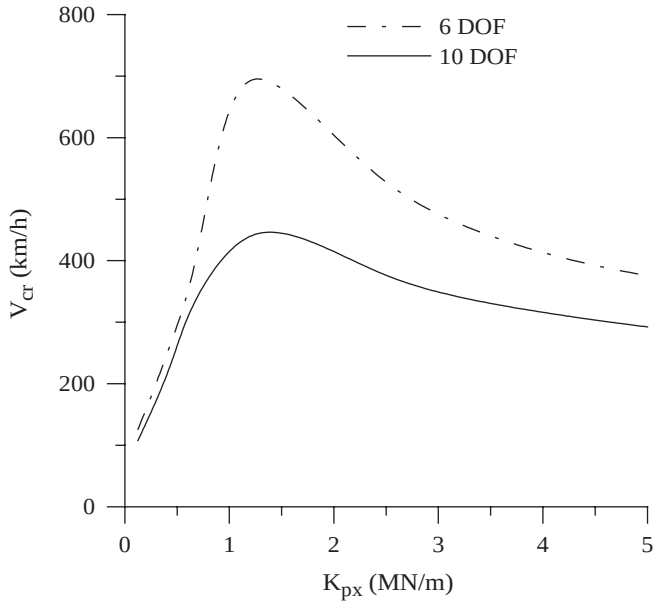

Fig. 6. Influence of longitudinal stiffness of primary suspension K_{px} on critical hunting speed of a truck evaluated via the six-DOF and 10-DOF systems ($\lambda=0.05$, $K_{py}=3.9\times10^5$ N/m, $K_{pz}=4.32\times10^5$ N/m, $C_{pz}=3\times10^4$ N s/m, $C_{sx}=9\times10^4$ N s/m, $C_{sy}=1.8\times10^3$ N s/m).

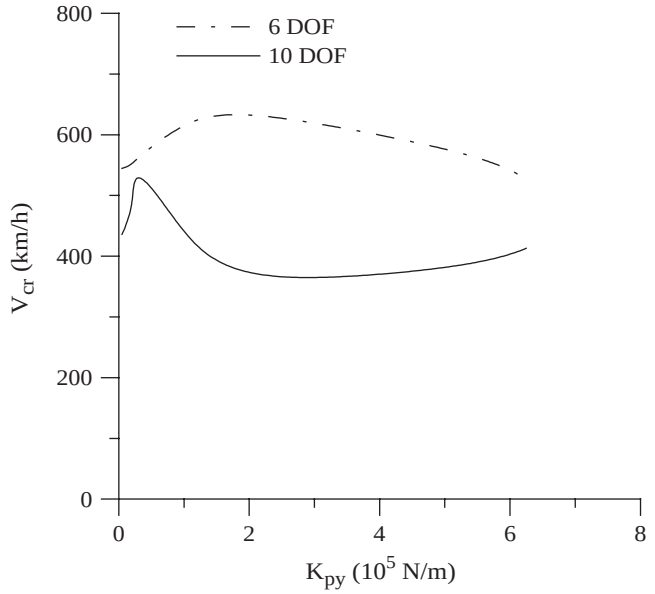

Fig. 7. Influence of lateral stiffness of primary suspension K_{py} on cirtical hunting speed of a truck evaluated via the six-DOF and 10-DOF systems ($\lambda = 0.05$, $K_{px} = 9 \times 10^5$ N/m, $K_{pz} = 4.32 \times 10^5$ N/m, $C_{pz} = 3 \times 10^4$ N s/m, $C_{sx} = 9 \times 10^4$ N s/m, $C_{sy} = 1.8 \times 10^3$ N s/m).

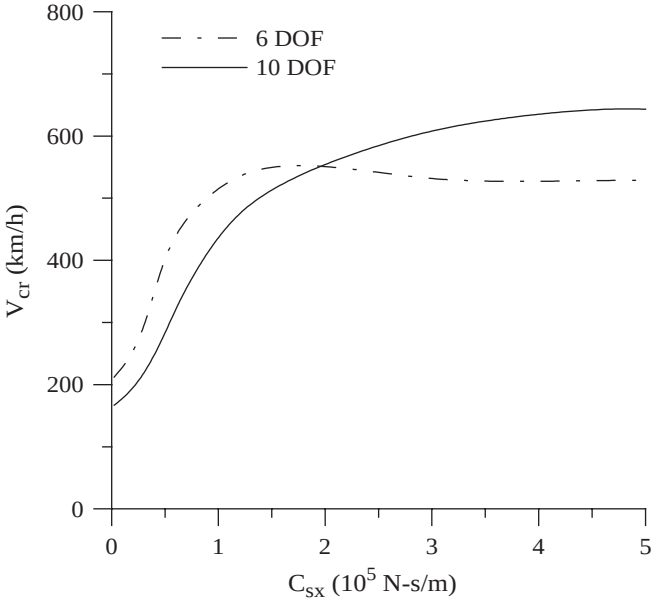

Fig. 8. Influence of longitudinal damping of secondary suspension C_{sx} on critical hunting speed of a truck evaluated via the six-DOF and 10-DOF systems ($\lambda = 0.05$, $K_{px} = 9 \times 10^5$ N/m, $K_{py} = 3.9 \times 10^5$ N/m, $K_{pz} = 4.32 \times 10^5$ N s/m, $C_{pz} = 3 \times 10^4$ N s/m, $C_{sy} = 1.8 \times 10^3$ N s/m).

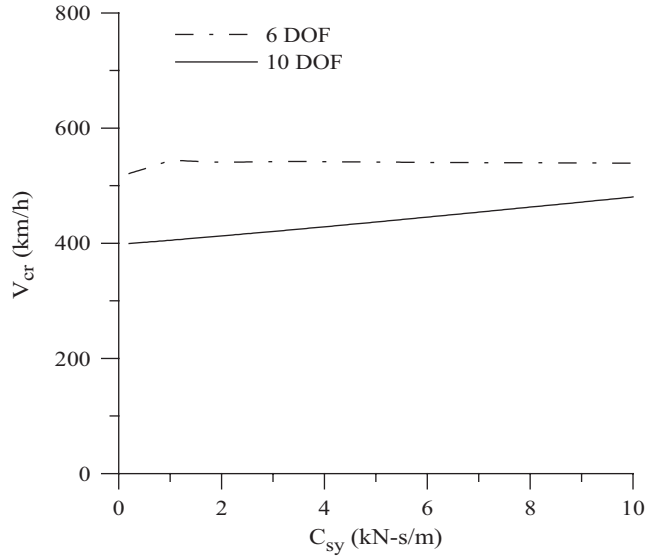

Fig. 9. Influence of lateral damping of secondary suspension C_{sy} on critical hunting speed of a truck evaluated via the six-DOF and 10-DOF systems ($\lambda = 0.05$, $K_{px} = 9 \times 10^5$ N/m, $K_{py} = 3.9 \times 10^5$ N/m, $K_{pz} = 4.32 \times 10^5$ N s/m, $C_{pz} = 3 \times 10^4$ N s/m, $C_{sx} = 9 \times 10^4$ N s/m).

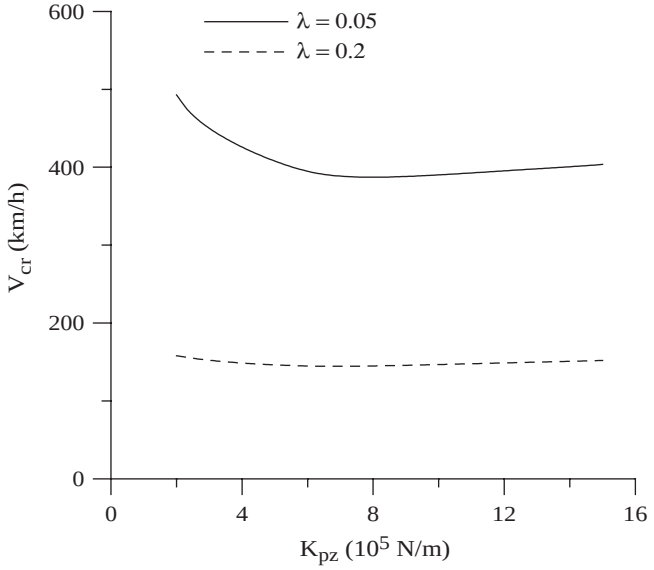

Fig. 10. Influence of vertical stiffness of primary suspension K_{pz} on critical hunting speeds evaluated for various wheel conicities ($K_{px} = 9 \times 10^5$ N/m, $K_{py} = 3.9 \times 10^5$ N/m, $C_{pz} = 3 \times 10^4$ N s/m, $C_{sx} = 9 \times 10^4$ N s/m, $C_{sy} = 1.8 \times 10^3$ N s/m).

It is noted that the vertical stiffness and the vertical damping of the primary suspension are not considered in either the six-DOF system or the 10-DOF system. A review of the available literature reveals that the influences of these two physical parameters on the critical hunting

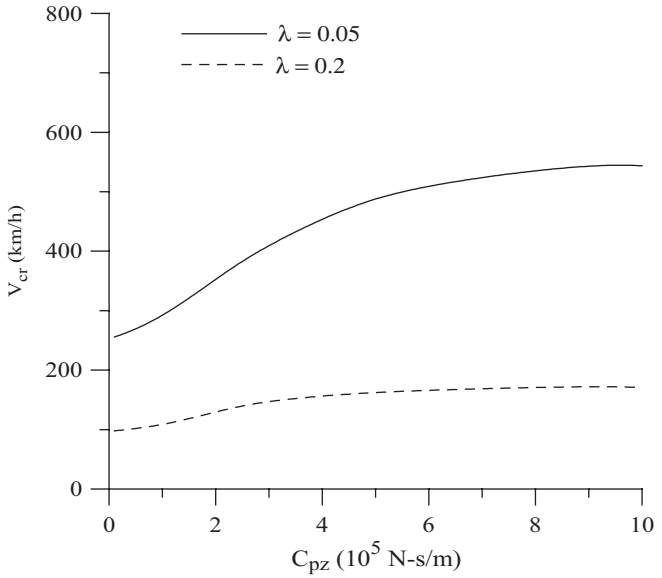

Fig. 11. Influence of vertical damping of primary suspension C_{pz} on critical hunting speeds evaluated for various wheel conicities ($K_{px}=9\times10^5$ N/m, $K_{py}=3.9\times10^5$ N/m, $K_{pz}=4.32\times10^5$ N/m, $C_{sx}=9\times10^4$ N s/m, $C_{sy}=1.8\times10^3$ N s/m).

speeds of the system have not been considered by previous researchers. Accordingly, Fig. 10 illustrates the influence of the vertical stiffness of the primary suspension, K_{pz}, on the critical hunting speeds of the truck for wheel conicities of 0.05 (new wheel tread) and 0.2 (old or worn wheel tread). The results indicate that for a truck with a new wheel tread, the critical hunting speed initially decreases as K_{pz} is increased, and then increases slightly as K_{pz} is further increased. Meanwhile, for the case of a worn wheel tread, the value of K_{pz} is seen to have only marginal influence on the critical hunting speed.

Fig. 11 shows the influence of the vertical damping of the primary suspension, C_{pz}, on the critical hunting speeds for wheel conicities of 0.05 and 0.2. The results demonstrate that in both cases, the critical hunting speed increases as the vertical damping of the primary suspension is increased.

The results of Figs. 10 and 11 reveal that the critical hunting speed of the truck decreases when the railway vehicle has been in service for an extended period of time.

5. Conclusions

This paper has employed a 10-DOF system to derive the linear governing differential equations of motion for a truck moving on tangent tracks. It has been shown that in most cases the critical hunting speeds evaluated by the six-DOF system are higher than those evaluated from the 10-DOF system. Furthermore, the results have shown that the critical hunting speed for a truck with new wheel treads is greater than that of a truck with old or worn wheel treads. The influences

of the vertical stiffness and vertical damping of the primary suspension, which are not considered in the six-DOF system, on the critical hunting speeds have also been investigated.

Acknowledgement

The present authors gratefully acknowledge the financial assistance provided to this study by the National Science Council of Taiwan, ROC under Grant No. NSC90-2212-E006-105.

Appendix A. Data of the system parameters [16,17]

Parameters	Value
Wheelset mass	$m_w = 1117.9\,\text{kg}$
Bogie frame mass	$m_t = 350.26\,\text{kg}$
Roll moment of the inertia of the wheelset	$I_{wx} = 608.1\,\text{kg m}^2$
Spin moment of the inertia of the wheelset	$I_{wy} = 72\,\text{kg m}^2$
Yaw moment of the inertia of the wheelset	$I_{wz} = 608.1\,\text{kg m}^2$
Yaw moment of the inertia of the bogie frame	$I_{tz} = 105.2\,\text{kg m}^2$
Wheel radius	$r_0 = 0.43\,\text{m}$
Half of the track gauge	$a = 0.7175\,\text{m}$
Wheel conicity	$\lambda = 0.05$
Half of the primary longitudinal spring arm	$b_1 = 1.0\,\text{m}$
Half of the primary longitudinal damping arm	$b_1 = 1.0\,\text{m}$
Half of the primary vertical spring arm	$b_1 = 1.0\,\text{m}$
Half of the primary vertical damping arm	$b_1 = 1.0\,\text{m}$
Half of the secondary longitudinal spring arm	$b_2 = 1.18\,\text{m}$
Half of the secondary longitudinal damping arm	$b_3 = 1.4\,\text{m}$
Half of the primary lateral spring arm	$L_1 = 1.28\,\text{m}$
Half of the primary lateral damping arm	$L_2 = 1.5\,\text{m}$
Vertical distance from the wheelset center of the gravity to the secondary suspension	$h_T = 0.47\,\text{m}$
Longitudinal stiffness of the primary suspension	$K_{px} = 9 \times 10^5\,\text{N/m}$
Lateral stiffness of the primary suspension	$K_{py} = 3.9 \times 10^5\,\text{N/m}$
Vertical stiffness of the primary suspension	$K_{pz} = 4.32 \times 10^5\,\text{N/m}$
Vertical damping of the primary suspension	$C_{pz} = 3 \times 10^4\,\text{N s/m}$
Longitudinal stiffness of the secondary suspension	$K_{sx} = 4.5 \times 10^3\,\text{N/m}$
Lateral stiffness of the secondary suspension	$K_{sy} = 4.5 \times 10^3\,\text{N/m}$
Longitudinal damping of the primary suspension	$C_{sx} = 9 \times 10^4\,\text{N s/m}$
Lateral damping of the primary suspension	$C_{sy} = 1.8 \times 10^3\,\text{Ns/m}$
Lateral rail stiffness	$K_r = 1.617 \times 10^7\,\text{N/m}$
Flange clearance	$\delta = 0.00923\,\text{m}$

Wheel flange height	$h_f = 30\,\text{mm}$
Lateral creep force coefficient	$f_{11} = 2.212 \times 10^6\,\text{N}$
Lateral/spin creep force coefficient	$f_{12} = 3120\,\text{N m}^2$
Spin creep force coefficient	$f_{22} = 16\,\text{N}$
Longitudinal creep force coefficient	$f_{33} = 2.563 \times 10^6\,\text{N}$
Axle load	$W = 5.6 \times 10^4\,\text{N}$

References

[1] R.V. Dukkipati, V.K. Garg, *Dynamics of Railway Vehicle Systems*, Academic Press, Canada, 1984.
[2] E.H. Law, N.K. Cooperrider, A survey of railway vehicle dynamics research, *Journal of Dynamic Systems, Measurement, and Control* (June 1974) 132–146.
[3] A.H. Wickens, The hunting stability of railway vehicle wheelsets and bogies having profiled wheels, *International Journal of Solids and Structures* 1 (1965) 319–341.
[4] A.H. Wickens, Static and dynamic instabilities of bogie railway vehicles with linkage steered wheelsets, *Vehicle System Dynamics* 26 (1996) 1–16.
[5] A.M. Whitman, On the lateral stability of a flexible truck, *Journal of Dynamic Systems, Measurement, and Control* 105 (1983) 120–125.
[6] A.M. Whitman, J.E. Molyneux, Limit cycle behavior of a flexible truck, *Journal of Applied Mechanics* 54 (1987) 930–934.
[7] R.V. Dukkipati, S. Narayana Swamy, M.O.M. Osman, Comparative performance of unconventional railway trucks, *International Journal of Vehicle Design* 19 (3) (1998) 326–339.
[8] D. Horak, D.N. Wormley, Nonlinear stability and tracking of rail passenger trucks, *Journal of Dynamic Systems, Measurement, and Control* 104 (1982) 256–263.
[9] M. Nó, J.K. Hedrick, High speed stability for rail vehicles considering varying conicity and creep coefficients, *Vehicle Systems Dynamics* 13 (1984) 299–313.
[10] J. Piotrowski, Stability of freight vehicles with the H-frame 2-axle cross-braced bogies. Simplified theory, *Vehicle Systems Dynamics* 17 (1988) 105–125.
[11] I. Haque, J. Lieh, A study of parametric stability of railway vehicles, *International Journal of Vehicle Design* 14 (2/3) (1993) 246–260.
[12] S. Narayana Swamy, R.V. Dukkipati, M.O.M. Osman, A comparative study on lateral stability and steady state curving behavior of unconventional rail truck models, *Proceedings of IMechE Part F: Journal of Rail and Rapid Transit* 208 (1994) 1–13.
[13] R.V. Dukkipati, S. Narayana Swamy, Lateral stability and steady state curving performance of unconventional rail trucks, *Mechanism and Machine Theory* 36 (2001) 577–587.
[14] A. Mehdi, Y. Shaopu, Effect of system nonlinearities on locomotive bogie hunting stability, *Vehicle System Dynamics* 29 (1998) 366–384.
[15] M. Vidyasager, *Nonlinear Systems Analysis*, Prentice-Hall, Englewood Cliffs, NJ, 1978.
[16] A.K.W. Ahmed, S. Sankar, Lateral stability behavior of railway freight car system with elasto-damper coupled wheelset: Part 2—truck model, *Journal of Mechanisms, Transmissions, and Automation in Design* 109 (4) (1987) 500–507.
[17] T. Hirotsu, K. Terada, M. Hiraishi, S. Yui, Simulation of hunting of rail vehicles (the case using a compound circular wheel profile), *JSME International Journal Series III, Vibration, Control Engineering, Engineering for Industry* 34 (3) (1991) 396–403.